Hydrogen bond dynamics in liquid methanol

4 AUTHORS, INCLUDING:

Gianni Cardini
University of Florence
171 PUBLICATIONS **2,374** CITATIONS

SEE PROFILE

Roberto Righini
University of Florence
171 PUBLICATIONS **4,041** CITATIONS

SEE PROFILE

Vincenzo Schettino
University of Florence
195 PUBLICATIONS **3,494** CITATIONS

SEE PROFILE

Hydrogen bond dynamics in liquid methanol

Marco Pagliai
*Laboratorio di Spettroscopia Molecolare, Dipartimento di Chimica, Università di Firenze,
Via della Lastruccia 3, 50019 Sesto Fiorentino, Firenze, Italia*

Gianni Cardini,[a] Roberto Righini, and Vincenzo Schettino
*Laboratorio di Spettroscopia Molecolare, Dipartimento di Chimica, Università di Firenze,
Via della Lastruccia 3, 50019 Sesto Fiorentino, Firenze, Italia and European Laboratory for Nonlinear
Spectroscopy (LENS), via Nello Carrara 1, 50019 Sesto Fiorentino, Firenze, Italia*

A Car–Parrinello molecular dynamics simulation has been performed on fully deuterated liquid
methanol. The results are compared with the latest available experimental and theoretical data. It is
shown that the liquid is aggregated in chains of hydrogen bonded molecules. The structure of the
aggregates is characterized and it is found that the dynamics includes a fast and a slow regime. The
weak H bond formed by the methyl group hydrogens and oxygen atom of surrounding molecules
has been characterized. The importance of inductive effects is shown and discussed in terms of
maximally localized Wannier function centers. Special attention is devoted to clarify how the
molecular dipole moment depends on the number of H bonds formed by each molecule. The IR
spectrum is computed and analyzed in terms of H-bond interactions. Insights on the short time
dynamics and on the H-bond network are illustrated. © *2003 American Institute of Physics.*
[DOI: 10.1063/1.1605093]

I. INTRODUCTION

There is a wide interest in the structural and dynamic
properties of liquid methanol both as a prototype of the large
category of alcohols and for its widespread applications as a
solvent in organic synthesis, in biochemistry, and
biotechnology.[1] As is the case for water, the structure of liq-
uid methanol is dominated by the formation of hydrogen
bonded networks. However, the presence of the methyl
group produces significant differences between water and
methanol.[1] In the former, tetrahedrally coordinated tridimen-
sional networks are present while methanol molecules are
bounded into linear chains that, sometimes, are interrupted
by the presence of bifurcations[1–5] as shown in Fig. 1.

Extensive information on the structural, dynamic and
spectroscopic properties of liquid methanol have been made
available from neutron[2,3,5] and x-ray scattering,[4] from
nuclear magnetic resonance,[6] IR, and Raman spec-
troscopies[7–9] and, in more recent years, also from femtosec-
ond time resolved experiments.[10,11] For the microscopic in-
terpretation of the experimental information an important
contribution has been given by modeling of the liquid
structure.[1] Starting from the 1980s, many computer
simulations[12–17] have been performed to rationalize and elu-
cidate the experimental findings. Early works in the area
were based on the development of accurate semiempirical
potentials that found application both in Monte Carlo[14–17]
and molecular dynamics (MD) simulations.[12,13] These al-
lowed one to reach a good understanding of the structure and
dynamics of liquid methanol, but several details of the hy-

drogen bonding array and of polarization interactions can
still be considered an open question.

The role of polarization in strongly self-associating liq-
uids has been stressed in several cases and attempts have
been made to develop model potentials including these
effects.[18] For instance, recently some of us[19] reported on a
conventional molecular dynamics study of liquid methanol
where induction effects on the optical spectra were modeled
through the application of the chemical potential equalization
method.[20–25] However, very recently a number of *ab initio*
molecular dynamics simulations[26–28] have been dedicated to
liquid methanol and these appear as the most appropriate
approach to fully take into account polarization effects and
intramolecular anharmonicity. In addition, recently a quan-
tum mechanical/molecular mechanical (QM/MM) model has
been proposed to overcome the size and time limit of *ab
initio* simulations by Morrone and Tuckerman.[29] The purpose
of the present paper is to extend the Car–Parrinello *ab initio*
molecular dynamics (CPMD)[30,31] simulations to fully deuter-
ated methanol to analyze in particular issues like the dynam-
ics of the hydrogen bonded network, including the estimate
of the hydrogen bond lifetime, the molecular dipole moment
in the associated liquid, and the vibrational and infrared
spectra.

II. COMPUTATIONAL DETAILS

The simulations have been performed with the CPMD
code[30] in a cubic box of 12.05 Å side, with periodic bound-
ary conditions and 26 methanol molecules. This choice cor-
responds to a sample density of 0.888 g cm^{-3} in good agree-
ment with the experimental one[7] at ambient temperature.
Martins–Troullier[32] pseudopotentials have been used along
with the Kleinman–Bylander[33] decomposition, and the plane
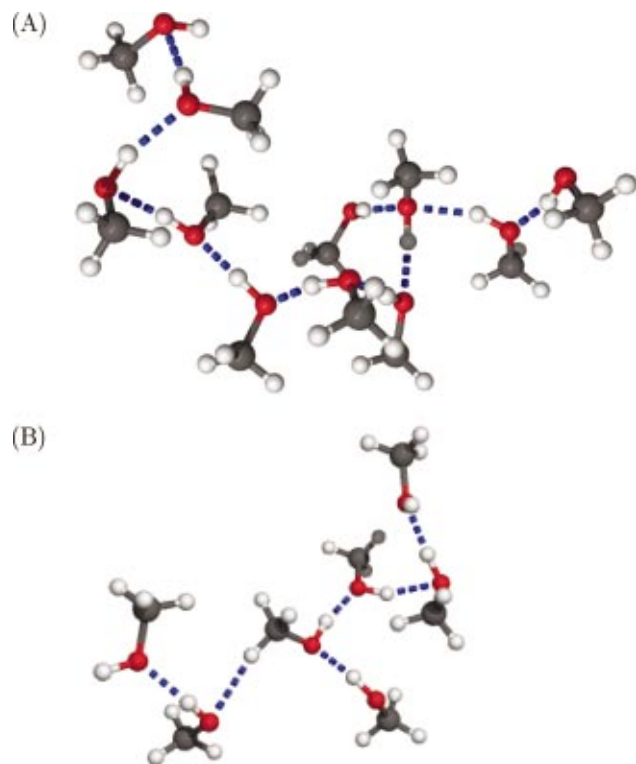
[a]Electronic mail: gianni.cardini@unifi.it

FIG. 1. (Color) Snapshot of methanol molecules bonded into a linear chain. (A) A bifurcation can be noted. (B) A hydrogen bond formed by the methyl group can be observed.
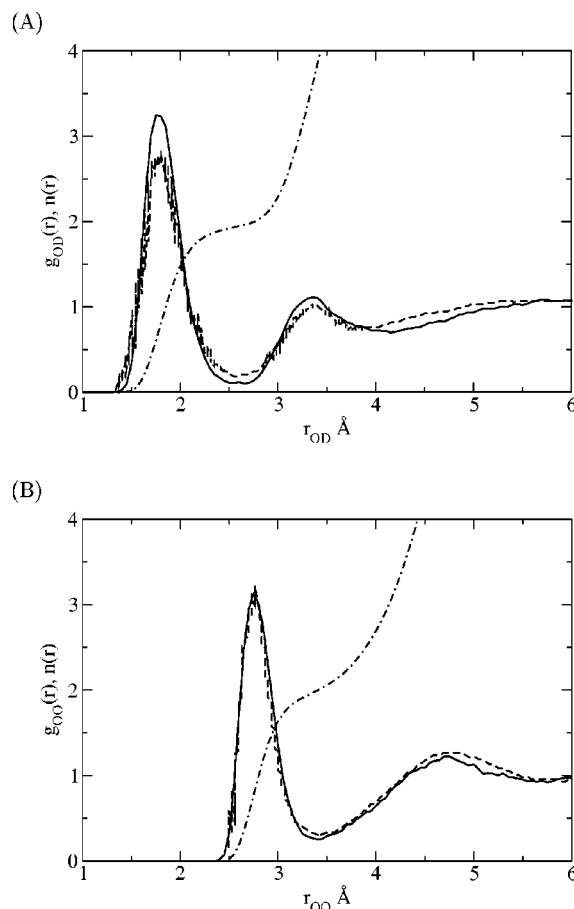

FIG. 2. (A) Radial distribution function (full) and running integration number (dash-dotted) for the OD intermolecular contacts. (B) Radial distribution function (full) and running integration number (dash-dotted) for the OO intermolecular contacts. The experimental radial distribution functions (dashed line) are taken from Yamaguchi *et al.* (Refs. 2 and 3).

wave expansions have been truncated at 70 Ry. Density functional calculations in the generalized gradient approximation (GGA) approximation have been performed using the BLYP[34,35] exchange correlational functional. The deuterium has been utilized instead of hydrogen to allow for a larger time step. A ficticious electronic mass of 800 a.u. has been adopted to keep the system on the Born–Oppenheimer surface.

Starting from a configuration extracted from a trajectory of a previous classical simulation,[19] and after 3 ps of thermalization at 300 K by velocity scaling followed by 2 ps of free dynamics, the equation of motions have been integrated with a time step of 5 a.u. ($\sim$0.12 fs) for a total simulation time of $\sim$17 ps in the *NVE* ensemble, storing the cell dipole and the atomic coordinates and velocities every five steps for the subsequent analysis.

During the simulation the total dipole moment of the cell, M, has been computed using the Berry phase scheme.[36–38] The infrared spectra (IR) have been obtained by the following relation:

$$I(\omega)=\omega^2\int_{-\infty}^{+\infty}e^{-i\omega t}\langle M(t)\cdot M(0)\rangle dt, \quad (1)$$

where $I(\omega)$ is the infrared intensity.[39]

The dipole moment of liquid methanol-d_4 has been obtained from the maximally localized Wannier function centers:[40,41]

$$x_i=-\frac{L}{2}\text{Im}\langle\omega_i|\exp(-i2x/L)|\omega_i\rangle, \quad (2)$$

where L is the cell dimension in the x direction (analogous definitions hold along y and z), ω_i is the ith Wannier function and $\langle...\rangle$ indicates the expectation values.

III. RESULTS

The accuracy of the simulation discussed in this paper can be stated by comparing the calculated and experimental[2,3] radial distribution functions (RDFs) that provide an averaged description of the surrounding of each molecule, and therefore represent the starting point for the analysis of the structure and stability of the H-bond network that characterizes liquid methanol.

The most interesting RDFs are those related to the hydrogen bond interaction. The $g_{OO}(r)$ and the $g_{OD}(r)$ pair radial distribution functions are shown in Fig. 2 along with the running integration number. The agreement between the experimental[2,3] and simulation results is excellent. From the integral up to the first minimum a value of the mean number of hydrogen bonds per molecule, $\langle n_{HB}\rangle$, of 2.0 and 1.9 from $g_{OO}(r)$ and $g_{OD}(r)$, respectively, is obtained. Owing to the directional character of the hydrogen bond interaction, the simple O$\cdots$H bond distance is not a sufficient criterion for its assessment.[42] As a matter of fact, more tight geometrical requirements have been suggested for the identification of
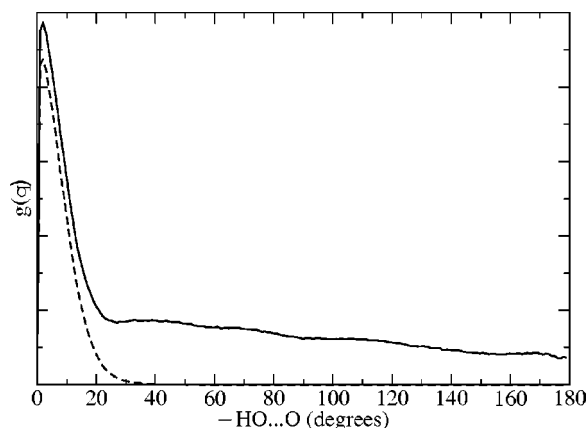
J. Chem. Phys., Vol. 119, No. 13, 1 October 2003

Hydrogen bond dynamics in methanol   6657

FIG. 3. Angular distribution functions of the DO···O angle. Continuum line: all the contacts. Dashed line: only O···O and O···D distances that satisfy the H-bond criteria.

FIG. 4. (Color) Number of molecules with zero, one, two, and three H bonds represented with orange, green, red, and blue colors, respectively.

hydrogen bonding in liquid methanol[12,13,43] and these include, beside the appropriately short distance between the hydrogen atom and the acceptor oxygen, a HO···O bond angle falling in a restricted range.[12,13,43] The following requirements should be verified

(1) $r(O···H)$ distance smaller than 2.6 Å,
(2) $r(O···O)$ distance smaller than 3.5 Å,
(3) $\angle HO···O$ angle smaller than 30°.

Even though the formation of hydrogen bonds should be discussed with reference to electronic structure and energetic parameters, the above-given geometrical criteria are very convenient to determine the structure and dynamics of associated networks since they can be directly related to the number of bonds per molecule at every time step of the simulation. In Fig. 3 the distribution of the $\angle DO···O$ angle for molecular pairs having O···D and O···O distances up to 2.6 and 3.5 Å, respectively, is shown. It can be seen that for bond distances satisfying the above-reported criteria the $\angle DO···O$ angle is definitively below 30°.

Using the geometrical criteria on the bond lengths and bond angle the function f_0, f_1, f_2, and f_3 representing the percentage of molecules involved in zero, one, two, and three hydrogen bonds, respectively, have been calculated along the simulation. These functions give an idea of the molecular connectivity in liquid methanol. Their variation during the simulation is shown in Fig. 4 and their average values are collected in Table I. On the whole the mean values of the f functions obtained in the present work agree qualitatively with previous estimates from other simulations.[13,27,44] However, the distinctly higher value of f_3 seems an indication of a larger complexity of the hydrogen bonded network (higher strength of H bond) than previously reported. If only a single type of linear chains of molecules were present in the liquid the approximately 7:2 ratio between f_2 and f_1 would imply the presence of chains of nine methanol molecules. A typical array of the hydrogen bonded methanol network obtained in the present work is shown in Fig. 1, where the presence of bifurcations can also be noted. From the f functions and following the procedure suggested
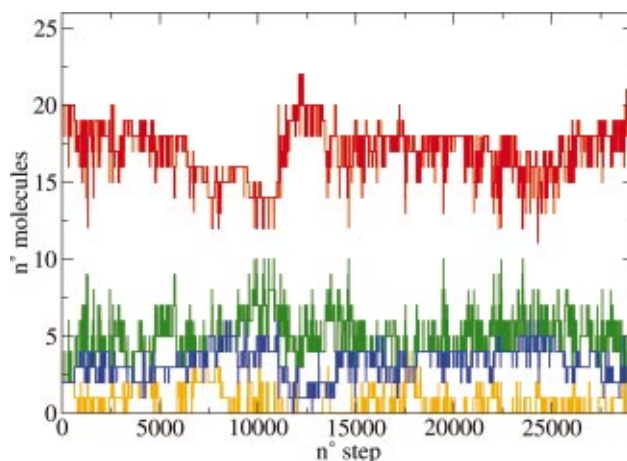
by Rapaport[45] a value of $\langle n_{HB} \rangle$ of 1.89 is obtained. As can be seen from Table I, this is in very good agreement with experiments[2,3] and with the results of previous simulations[13,27,44] as well.

To enlighten the dynamics of the hydrogen bond formation it is useful to define and calculate a lifetime of the hydrogen bond, τ_{HB}. To this purpose one could define at every time step t and for each H···O contact, labeled with j, a function

$$H_j(t) = \delta(H - \text{bond}) \qquad (3)$$

that takes the value of 1 if the adopted geometrical criteria for the hydrogen bond formation are fulfilled and the value of 0 otherwise. However, such a simple function has the drawback of a strong discontinuity and, in addition, does not take into account the effect of molecular vibrations. To overcome these problems, in a previous work[46] the more flexible function

$$F_j(t) = A(r(t)) \cdot B(\theta(t)) \qquad (4)$$

has been introduced where $A(r(t))$ and $B(\theta(t))$ are defined as

$$
\begin{aligned}
A(r(t)) &= e^{-(r_e - r_j(t))^2/(2\sigma_r^2)} \quad \text{if } (r_e - r_j(t)) < 0, \\
A(r(t)) &= 1 \quad \text{if } (r_e - r_j(t)) \geq 0, \\
B(\theta(t)) &= e^{-(\theta_e - \theta_j(t))^2/(2\sigma_\theta^2)} \quad \text{if } (\theta_e - \theta_j(t)) < 0, \\
B(\theta(t)) &= 1 \quad \text{if } (\theta_e - \theta_j(t)) \geq 0
\end{aligned} \qquad (5)
$$

and r_e and θ_e are the positions of the first peak in $g_{OD}(r)$ (see Fig. 2) and in $g(\theta)$ (see Fig. 3), respectively, whereas r_j and θ_j are the instantaneous values of these quantities and σ_r and σ_θ are the half-width at half-maximum of the peaks.

The calculated lifetime of the hydrogen bond obtained from the function (4) is reported in Table I. It can be seen that τ_{HB}, obtained from $F_j(t)$, is definitively larger than the value obtained from $H_j(t)$. This was to be expected since, using the $F_j(t)$ function, values of A and B close to one are also taken into account. It has been checked that the selected limiting value of the $F_j(t)$ function does not affect the cal-

TABLE I. Some salient properties of methanol: f_i labels the percentage of molecule involved in i hydrogen bonds, $\langle n_{HB} \rangle$ is the average number of H bonds, τ_{HB} is the H-bond lifetime, and μ is the average molecular dipole moment. Superscripts c and n refer to values obtained by Eqs. (3) and (4), respectively.

| | | Reference | | | | | | | | |
	This work	64		13			44	27	26	Expt.
f_0	3	1	4	1	1	0.1	1.72	4		
f_1	18	16.5	29	16	18	7	19.65	20		
f_2	66	75.5	59	76	72	90	71.91	67		
f_3	13	7	9	7	8	3	6.70	8		
$\langle n_{HB} \rangle$	1.89	1.9	1.73	1.89	1.87	1.96	1.84	1.79	1.6	$1.9^{2,3}$
τ_{HB} (ps)	1.29^c, 1.9^n	1.5	0.7	1.4	1.2	2.5	0.3, 0.9			$\sim 2^{63}$
μ (D)	2.64		2.20	2.22	2.33	2.37			2.54	

culated τ_{HB}. Evidence of this is also obtained considering that, as can be seen from Fig. 5, the $g(r, \theta)$ distribution function weighted by $H_j(t)$ or $F_j(t)$ extends over a similar phase space region.

In liquid water the $H_j(t)$ function, Eq. (3), has been used by Luzar and Chandler[47] to define the reactive flux function and to analyze whether the breaking and formation of hydrogen bonds are correlated. The short time duration of the present simulation and the sample dimension do not allow for such a complex analysis. However, the correlation function

$$c(t) = \frac{1}{N} \sum_j^N \frac{\langle F_j(0) F_j(t) \rangle}{\langle F_j(0) \rangle^2} \qquad (6)$$

that measures the hydrogen bond stability has been calculated and the results are reported in Fig. 6. The variation of $\ln[c(t)]$ with time appears to be nonlinear, suggesting that the dynamics of the hydrogen bond rearrangement include at least a slow and a fast process with characteristic times of 1.9 ± 0.1 and 0.5 ± 0.1 ps, respectively. It can be seen in the inset of Fig. 6 that at short times ($t \leqslant 1$ ps) the behavior is characterized by dumped oscillations very much like it has been reported for liquid water.[47,48] The wave number of the damped oscillation can be estimated to be ~ 1000 cm^{-1} and it is most likely a modulation due to the O–D···O libration motion. The long time behavior of the correlation function 6 should be associated with formation/breaking dynamics of the hydrogen bond. This type of analysis is consistent with the values of τ_{HB} discussed earlier, with an estimated lifetime close to 1.9 ps.

Recent spectroscopic studies[49] have suggested the presence of a weak directional interaction between the hydrogens of the methyl group and oxygen atom of neighboring molecules. The formation of this weak hydrogen bond is a topic of renewed interest[42] and has recently been discussed in various systems,[46,50] although it is not generally analyzed in MD simulations. In the case of liquid methanol the $g_{DO}(r)$ pair distribution function shows a small bump near 2.3 Å. This has been evidenced plotting the first derivative of the distributions function and this allowed us to obtain the parameters to be used in Eq. (4). The association of this feature with a weak directional interaction of the methyl hydrogens is clearly demonstrated by the weighted $g(r, \theta)$ function shown in Fig. 7. In a molecular dynamics simulation, a very similar interaction has been recently found[46] for the transition state

of the S_N2 reaction $Cl^- + CH_3Br$ in water with a lifetime of only 53 fs for the H bond between the oxygen atom of the solvent and the methyl group.

IV. MOLECULAR DIPOLE MOMENT

Strong intermolecular interactions, like the hydrogen bonding, are expected to induce a substantial rearrangement of the molecular electronic density that can be efficiently revealed by the variation of the molecular dipole moment in the condensed phase as compared to the isolated molecule. This effect has been reported in the case of water,[51–54] where it has also been shown that semiempirical potentials, even in the form of polarizable models, are unable to reproduce the actual changes of the dipole moment. The relevance of the polarization effects in hydrogen bonded water has been further demonstrated by the changes of the dipole moment in critical and supercritical water as compared to liquid water in standard conditions.[51,52,55,56]

Similar effects have been studied in liquid methanol calculating the molecular dipole moment by the maximally localized Wannier function centers method[40,41] and averaging over 293, equally spaced in time, configurations of the liquid sample. The results are reported in Fig. 8 where the contribution from molecules involved in zero, one, two, and three hydrogen bonds is also shown separately. It can be noted that almost Gaussian distributions are obtained. It is also seen that the mean dipole moment remarkably depends on the number of hydrogen bonds and values of 2.06, 2.24, 2.71, and 2.99 D are obtained for a number of zero, one, two, and three hydrogen bonds, respectively, with an average value of 2.64 D. The general trend observed in liquid methanol closely resembles results reported for water, for which an average value of 2.95 D of the molecular dipole moment has been found.[51,52,55,56] The mean value of the dipole moment is reported in Table I and compared with results of other simulations. It can be seen again that the present simulation seems to indicate stronger hydrogen bonds and an increased change of the electron distribution. The average value of the dipole moment obtained in this work differs by approximately 0.1 D from that obtained by Handgraaf et al.[26] for CH_3OH using the same Car–Parrinello approach. This difference can be due either to the slightly different density of the simulated samples and to the lower number of molecules or to the larger simulation time and number of configurations used in
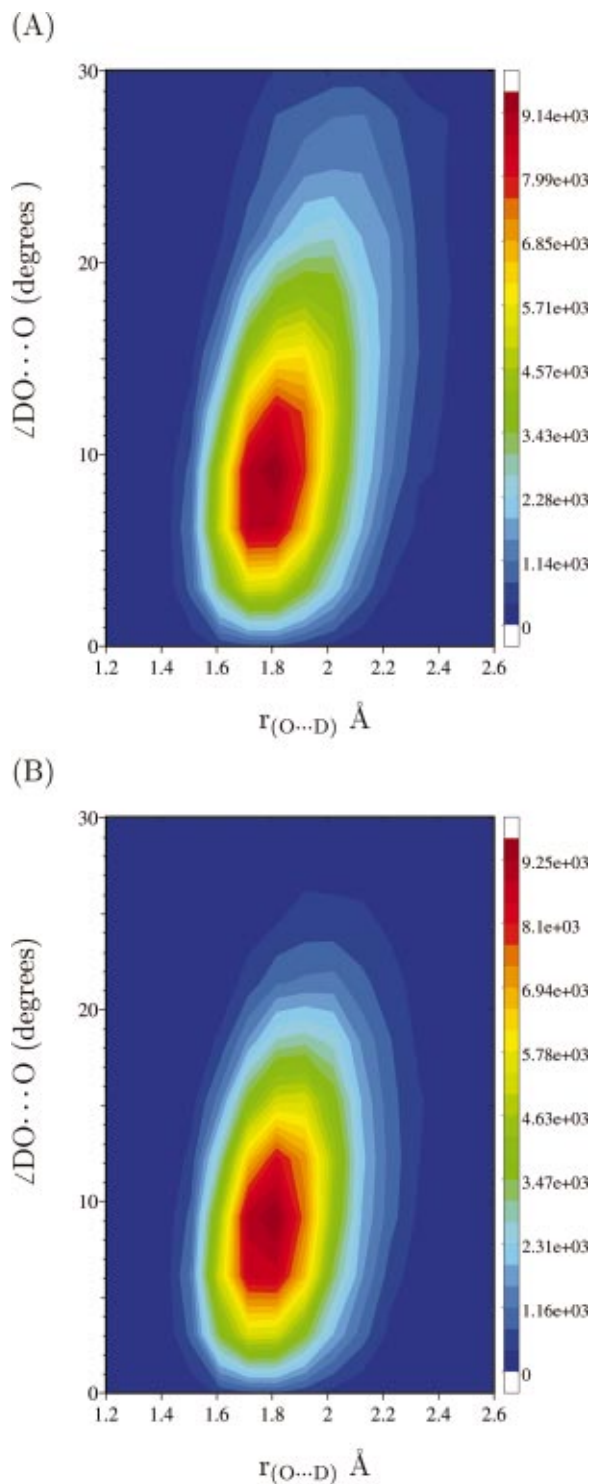
J. Chem. Phys., Vol. 119, No. 13, 1 October 2003

Hydrogen bond dynamics in methanol   6659

(A)

(B)

FIG. 5. (Color) $g(r,\theta)$ weighted functions for the DO$\cdots$O interactions obtained with classical criteria (A), and by Eq. (4)—(B).
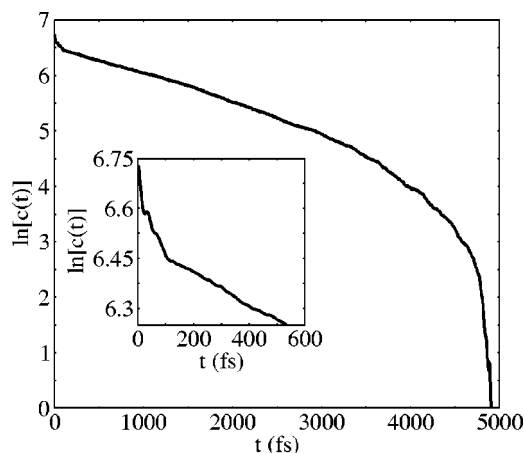

FIG. 6. H-bonds autocorrelation function [Eq. (6)]. The short time region is reported in the inset panel.

$$G_k = \frac{\langle \mathbf{M}^2 \rangle}{N_m \langle \mu^2 \rangle}, \tag{7}$$

where $\langle \mathbf{M}^2 \rangle$ is the average square dipole moment of the system, N_m is the number of molecules, and $\langle \mu^2 \rangle$ is the average square molecular dipole. The value of G_k obtained in the present work for methanol is 3.77 ± 1.70, in fairly good agreement with the experimental value, 2.94, reported by Kirkwood.[59] As already noticed by Ladanyi,[1] the large uncertainty is due to the limited length of the simulation that does not allow one to reach a fully converged value, as can be seen by an inspection of the running average of $\langle \mathbf{M}^2 \rangle$ shown in Fig. 9. This is not surprising since $\mathbf{M}^2$ is related to the dielectric constant, a quantity whose evaluation is well known to be very slowly convergent.[1]
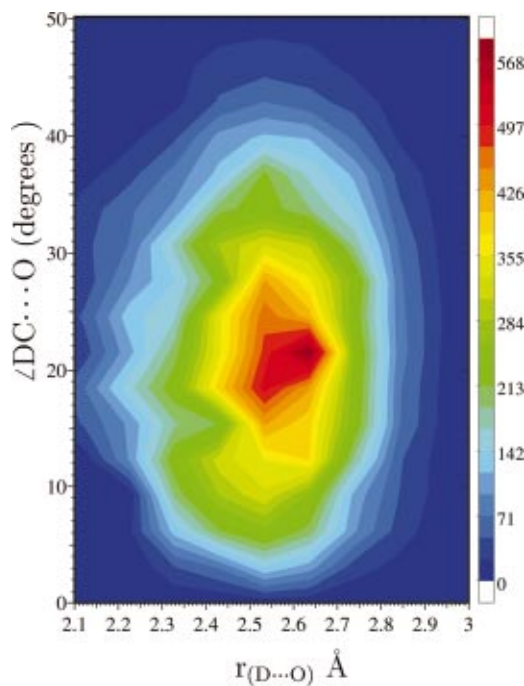

FIG. 7. (Color) $g(r,\theta)$ weighted functions for the CD$\cdots$O interactions obtained by Eq. (4).

this work or, also, to the effect of the deuterium isotope. However, the results, of the present work are in good agreement with estimates by Sum et al.[57,58] from a molecular dynamics simulation at 330 K using a polarizable intermolecular potential model fitted on accurate ab initio calculations. Usually, the orientational degree of a dipolar system can be described by the Kirkwood factor:

FIG. 10. Top panel: IR spectra of liquid methanol [Eq. (1)]. Lower panel: Experimental IR spectra: (A) from Ref. 39, (B) obtained in the present work with a FT-IR Bruker IFS 120 HR between KBr windows, (C) from Ref. 67. The intensities of the three experimental spectra are reported on different scales to evidence their features.
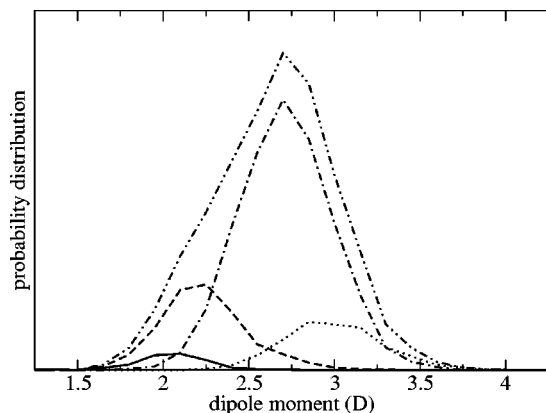

FIG. 8. Methanol dipole moment. The total dipole moment is represented with a double dot-dashed line. The dipole moment of the zero, one, two, and three H-bonds component is represented with full, dashed, dot-dashed and dotted line, respectively.

V. VIBRATIONAL AND INFRARED SPECTRA

The infrared absorption spectrum is a very sensitive probe of hydrogen bonding liquids.[60] As such the infrared spectrum of methanol and of its deuterated isotopes has been studied in considerable details experimentally[7,8] and the vibrational assignment of the internal modes is pretty well understood. Modeling of the infrared spectrum has, however, proved to be a difficult task, most likely because of difficulties in fully considering the polarization and anharmonicity effects on the vibrational frequencies and absorption coefficients. Recently a calculation of the infrared and Raman spectrum of methanol has been reported[19] taking into account the polarization effects on the absorption coefficient but not on the dynamics. Since the Car–Parrinello approach[31] actually considers both polarization and the anharmonicity terms an attempt has been made to calculate the infrared spectrum of liquid CD_3OD. The result is reported in Fig. 10. It can be seen that the agreement with experiments is quite satisfactory. In particular, it can be noted that the relative intensities of the prominent features observed at ~ 900 and ~ 1100 cm^{-1} are well reproduced in the calculation and
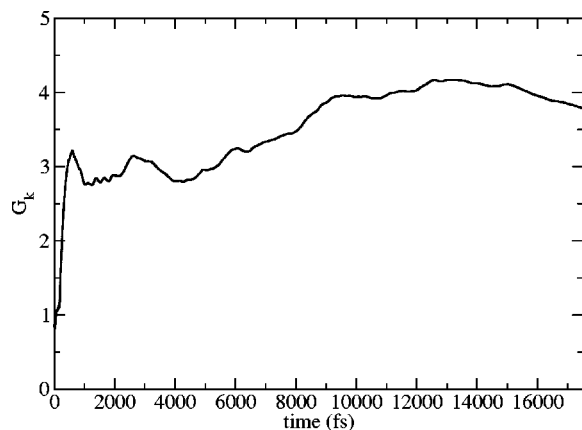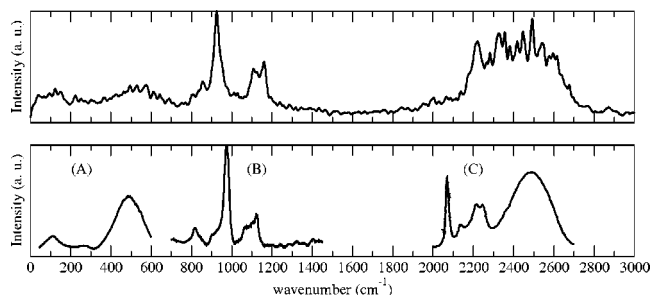

FIG. 9. Variation of the Kirkwood factor (Refs. 51 and 52) during the simulation.

this is a significant improvement compared to the previous paper by Chelli *et al.*[19] The agreement with experiment is on the whole satisfactory also in the OD and CD stretching region, considering that the small number of the molecules in the simulated sample makes the distribution of frequencies not smooth and that the neglect of the zero point energy reduces the anharmonicity of the system. The calculated vibrational frequencies of liquid deuterated methanol are compared with experiments in Table II, where the band assignment is also shown together with the calculated and observed frequencies of the isolated molecule. It can be seen, in particular, that the redshift of the OD stretching mode and the blueshift of the COD bending mode in the liquid are pretty well reproduced.

To analyze the spectrum in more detail the vibrational density of states has been obtained as the Fourier transform of the velocity autocorrelation function. The power spectrum obtained in this way has been decomposed and analyzed by computing the power spectra of the autocorrelation function of appropriate intramolecular and intermolecular coordinates.[61] The results for the intramolecular modes are shown in Fig. 11. It can be seen that, apart from the CD_3 and OD stretching modes, the mixing of the modes is considerable. In particular the mixing of the COD bending with low frequency modes should be noted. This and the already noted blueshift gives some intermolecular character to the COD bending mode. Also the heavy coupling of the torsional τ_{DCOD} mode with both the intra- and intermolecular modes should be remarked.

The power spectra of the selected intermolecular coordinates are shown in Fig. 12. The mixing of the modes point to the "collective" character of the motions in the hydrogen bond network. In agreement with Guillot *et al.*[39] and Passchier *et al.*,[62] this analysis of the power spectra suggest an assignment of the infrared feature at ~ 150 cm^{-1} as a libration around the CO bond and of the feature at ~ 280 cm^{-1} as the O$\cdots$O stretching mode. This latter assignment is further supported by the observed small frequency dependence on the isotopic substitution[7,8] and by the strong dependence on the temperature of its intensity.[62]

TABLE II. Experimental and theoretical gas and liquid phase infrared frequencies. As references gas phase unscaled frequencies are reported. (G=aug-cc-pVQZ basis set and plane wave (PW)=70 Ry cut-off) The BLYP/PW liquid frequencies have been scaled by 1.0975. The BLYP/PW gas phase frequencies have been obtained by linear response theory (Ref. 66).

	Gas			Liquid	
Assignment	Expt.[a]	B3LYP/G	BLYP/PW	Expt.[b]	BLYP/PW
DCOD torsion	196	249.43	191.2	485	526
COD bending	776	766.68	759.1	824	858
CD_3 deformation	892	881.73	875.8	902	910
CO stretching	983	961.10	907.6	979	940
CD_3 deformation	1024	1052.41	1035.3	1057	1095
CD_3 asym-bending	1060	1074.88	1060.7	1064	1125
CD_3 asym-bending	1080	1087.16	1070.1	1097	1140
CD_3 sym-bending	1135	1141.18	1093.7	1125	1170
CD_3 sym-stretching	2080	2086.26	2121.5	2072	2220
CD_3 asym-stretching	2228	2182.14	2229.0	2216	2350
CD_3 asym-stretching	2260	2254.74	2277.3	2245	2365
OD stretching	2724	2614.06	2633.6	2493	2580

[a]Reference 65.
[b]Reference 7.

VI. CONCLUSIONS

The results of an *ab initio* molecular dynamics simulation on the deuterated methanol at ambient temperature have been reported. The model has been preliminary shown to be able to reproduce with good accuracy the radial distribution functions obtained from x-ray[4] and inelastic neutron[2,3] diffraction data. The structure of the liquid is found to be made of hydrogen bonded chains with an average length including approximately ten methanol units. However, a significant number of methanol molecules are involved in three hydro-

gen bonds and this implies that bifurcations occur in the hydrogen bonded chains. The number of units not involved in any hydrogen bond is very limited. The complexity of the aggregation in the liquid is further enhanced by the presence
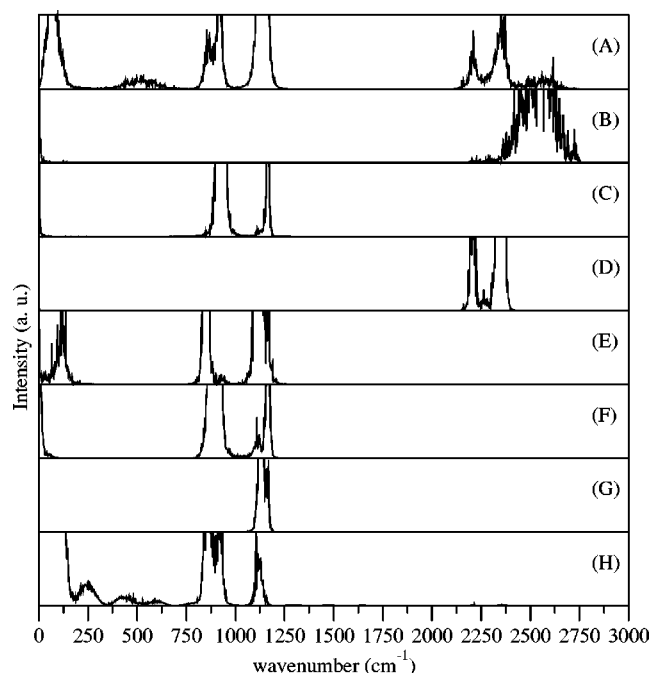

FIG. 11. Autocorrelation functions of the intramolecular modes. From top to bottom panel: (A) power spectra (PS) of the velocity autocorrelation function; (B) PS of the OD stretching mode; (C) PS of the CO stretching mode; (D) PS of the CD stretching mode; (E) PS of the COD bending mode; (F) PS of the DCD bending mode; (G) PS of the DCO bending mode; (H) PS of the DCOD torsion mode.
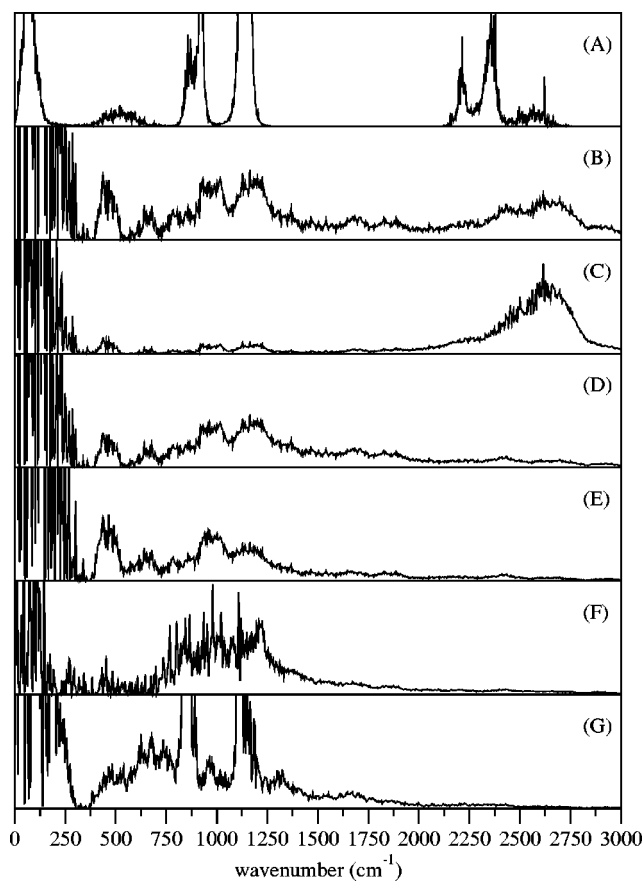

FIG. 12. Autocorrelation functions of the intermolecular modes. From top to bottom panel: (A) Power spectra (PS) of the velocity autocorrelation function; (B) PS of the D···O stretching mode; (C) PS of the OD···O antisymmetric stretching; (D) PS of the OD···O symmetric stretching mode; (E) PS of O···O stretching mode; (F) PS of the OD···O bending mode; (G) PS of the COD···O torsion mode.

of a weaker directional interaction between the methyl hydrogens and the oxygen atoms of neighboring molecules. The dynamics of the hydrogen bond has been characterized through the evaluation of the lifetime of the hydrogen bond that is estimated to be ~1.9 ps, in good agreement with recent experiments.[63] However, the dynamics includes a shorter time regime (~0.5 ps) that should be associated with a modulation due to in-plane or out-of-plane librations of the molecular pairs.

The polarization effects in the hydrogen bonded network has been studied in detail and in particular through the evaluation of the changes in the molecular dipole moment. This has been found to depend considerably on the number of hydrogen bonds in which the molecules is involved. On the average the dipole moment increases by 28% as a result of aggregation in the liquid. As a whole the results of the present work suggest that in semiempirical model potentials the polarization effects should be given a higher role than done so far. Similar conclusions have been reached in the case of the liquid water.[51,52,55,56] The reliability of the present form of the *ab initio* MD simulation has been confirmed by the calculation of the infrared absorption spectrum. The results have been found to reproduce with good accuracy the salient feature of the experimental spectrum.[7,8]

ACKNOWLEDGMENTS

[1] B. M. Ladanyi and M. S. Skaf, Annu. Rev. Phys. Chem. **44**, 335 (1993).
[2] T. Yamaguchi, K. Hidaka, and A. K. Soper, Mol. Phys. **96**, 1159 (1999).
[3] T. Yamaguchi, K. Hidaka, and A. K. Soper, Mol. Phys. **97**, 603 (1999).
[4] A. H. Narten and A. Habenschuss, J. Chem. Phys. **80**, 3387 (1984).
[5] T. Weitkamp, J. Neuefeind, H. E. Fischer, and M. D. Zeidler, Mol. Phys. **98**, 125 (2000).
[6] N. Asahi and Y. Nakamura, J. Chem. Phys. **109**, 9879 (1998).
[7] J. E. Bertie and S. L. Zang, Phys. Rev. B **37**, 785 (1988).
[8] J. E. Bertie and S. L. Zhang, J. Mol. Struct. **413–414**, 333 (1997).
[9] U. Buck and F. Huisken, Chem. Rev. (Washington, D.C.) **100**, 3863 (2000).
[10] H. Shirota, K. Yoshihara, N. A. Smith, S. Lin, and S. R. Meech, Chem. Phys. Lett. **281**, 27 (1997).
[11] N. A. Smith and S. R. Meech, Faraday Discuss. **108**, 35 (1997).
[12] M. Haughney, M. Ferrario, and I. R. McDonald, Mol. Phys. **88**, 849 (1986).
[13] M. Haughney, M. Ferrario, and I. R. McDonald, J. Phys. Chem. **91**, 4934 (1987).
[14] W. L. Jorgensen, J. Am. Chem. Soc. **102**, 543 (1980).
[15] W. L. Jorgensen, J. Am. Chem. Soc. **103**, 341 (1981).
[16] W. L. Jorgensen, J. Am. Chem. Soc. **103**, 335 (1981).
[17] W. L. Jorgensen, J. Phys. Chem. **90**, 1276 (1986).
[18] J. Gao, D. Habibollazadeh, and L. Shao, J. Phys. Chem. **99**, 16460 (1995).
[19] R. Chelli, S. Ciabatti, G. Cardini, R. Righini, and P. Procacci, J. Chem. Phys. **111**, 4218 (1999).
[20] D. M. York and W. Yang, J. Chem. Phys. **104**, 159 (1996).
[21] A. K. Rappe and W. A. Goddard, III, J. Phys. Chem. **95**, 3358 (1991).
[22] C. Bret, M. J. Field, and L. Hemmingsen, Mol. Phys. **98**, 751 (2000).
[23] W. J. Mortier, S. K. Ghosh, and S. Shankar, J. Am. Chem. Soc. **108**, 4315 (1986).
[24] P. Itskowitz and M. L. Berkowitz, J. Phys. Chem. A **101**, 5687 (1997).
[25] P. Itskowitz and M. L. Berkowitz, J. Phys. Chem. A **102**, 4808 (1998).
[26] J.-W. Handgraaf, T. S. van Erp, and E. J. Meijer, Chem. Phys. Lett. **367**, 617 (2003).
[27] E. Tsuchida, Y. Kanada, and M. Tsukada, Chem. Phys. Lett. **311**, 236 (1999).
[28] J. A. Morrone and M. E. Tuckerman, J. Chem. Phys. **117**, 4403 (2002).
[29] J. A. Morrone and M. E. Tuckerman, Chem. Phys. Lett. **370**, 406 (2003).
[30] J. Hutter, A. Alavi, T. Deutch, M. Bernasconi, S. Goedecker, D. Marx, M. Tuckerman, and M. Parrinello, CPMD, MPI für Festkörperforschung and IBM Zurich Research Laboratory, Stuttgart, 1995–1999.
[31] R. Car and M. Parrinello, Phys. Rev. Lett. **55**, 2471 (1985).
[32] N. Troullier and J. L. Martins, Phys. Rev. B **43**, 1993 (1991).
[33] L. Kleinman and D. M. Bylander, Phys. Rev. Lett. **48**, 1425 (1982).
[34] A. D. Becke, Phys. Rev. A **38**, 3098 (1988).
[35] C. Lee, W. Yang, and R. G. Parr, Phys. Rev. B **37**, 785 (1988).
[36] J. S. Tse, Annu. Rev. Phys. Chem. **53**, 249 (2002).
[37] R. Resta, Rev. Mod. Phys. **66**, 899 (1994).
[38] D. Vanderbilt and R. D. King-Smith, Phys. Rev. B **48**, 4442 (1993).
[39] B. Guillot, P. Marteau, and J. Obriot, J. Chem. Phys. **93**, 6148 (1990).
[40] N. Marzari and D. Vanderbilt, Phys. Rev. B **56**, 12847 (1997).
[41] P. L. Silvestrelli, N. Marzari, D. Vanderbilt, and M. Parrinello, Solid State Commun. **107**, 7 (1998).
[42] G. R. Desiraju and T. Steiner, *The Weak Hydrogen Bond* (Oxford University Press, New York, 1999).
[43] P. Sindzingre and M. L. Klein, J. Chem. Phys. **96**, 4681 (1992).
[44] M. Matsumoto and K. E. Gubbins, J. Chem. Phys. **93**, 1981 (1990).
[45] D. C. Rapaport, Mol. Phys. **50**, 1151 (1983).
[46] M. Pagliai, S. Raugei, G. Cardini, and V. Schettino, J. Mol. Struct.: THEOCHEM **630**, 141 (2003).
[47] A. Luzar and D. Chandler, Phys. Rev. Lett. **76**, 928 (1996).
[48] F. W. Starr, J. K. Nielsen, and H. E. Stanley, Phys. Rev. Lett. **82**, 2294 (1999).
[49] G. V. Yukhnevich and E. G. Tarakanova, J. Mol. Struct. **447**, 257 (1998).
[50] M. Hartmann, S. D. Wetmore, and L. Radom, J. Phys. Chem. A **105**, 4470 (2001).
[51] M. Boero, K. Terakura, T. Ikeshoji, C. C. Liew, and M. Parrinello, Phys. Rev. Lett. **85**, 3245 (2000).
[52] M. Boero, K. Terakura, T. Ikeshoji, C. C. Liew, and M. Parrinello, J. Chem. Phys. **115**, 2219 (2001).
[53] L. Delle Site, A. Alavi, and R. M. Lynden-Bell, Mol. Phys. **96**, 1683 (1999).
[54] L. Delle Site, A. Alavi, and R. M. Lynden-Bell, J. Mol. Liq. **98–99**, 79 (2002).
[55] P. L. Silvestrelli and M. Parrinello, Phys. Rev. Lett. **82**, 3308 (1999).
[56] P. L. Silvestrelli and M. Parrinello, J. Chem. Phys. **111**, 3572 (1999).
[57] A. K. Sum, S. I. Sandler, R. Bukowski, and K. Szalewicz, J. Chem. Phys. **116**, 7627 (2002).
[58] A. K. Sum, S. I. Sandler, R. Bukowski, and K. Szalewicz, J. Chem. Phys. **116**, 7637 (2002).
[59] G. Oster and J. G. Kirkwood, J. Chem. Phys. **11**, 175 (1943).
[60] J. Martí, J. A. Padró, and E. Guàrdia, J. Mol. Liq. **64**, 1 (1995).
[61] G. Cardini and V. Schettino, Chem. Phys. **146**, 147 (1990).
[62] W. F. Passchier, R. Klopmaker, and M. Mandel, Chem. Phys. Lett. **4**, 485 (1970).
[63] K. J. Gaffney, P. H. Davis, I. R. Piletic, N. E. Levinger, and M. D. Fayer, J. Phys. Chem. A **106**, 12012 (2002).
[64] J. A. Padró, L. Saiz, and E. Guàrdia, J. Mol. Struct. **416**, 243 (1997).
[65] NIST, http://webbook.nist.gov (2003).
[66] A. Putrino, D. Sebastiani, and M. Parrinello, J. Chem. Phys. **113**, 7102 (2000).
[67] B. Schrader, *Raman/Infrared Atlas of Organic Compounds* (VCH, New York, 1989).